Contribution from the Savannah River Laboratory,
E. I. du Pont de Nemours and Company, Aiken, South Carolina 29808

Oxidation of Hydrazine by Nitric Acid†

David G. Karraker

Received January 7, 1985

Hydrazine is oxidized by hot nitric acid in a first-order reaction to produce N_2, N_2O, HN_3, and NH_4^+. The rate law for the reaction is $-d \ln (N_2H_4)/dt = k(NO_3^-)(H^+)^2$ where $k = 5.8 \times 10^{-5}$ M^{-3} min^{-1} at 100 °C in 5.44 M HNO_3 and $\mu = 6$. The data are consistent with a reaction mechanism that involves HN_3, HNO_2, and the N_2H_2 free radical as intermediates and N_2, N_2O, and NH_4^+ as products. The Arrhenius equation constants over the temperature range 70–100 °C were $A = 1.2 \times 10^{11}$ M^{-3} min^{-1} and $E = 26$ kcal/mol. The reaction is catalyzed by Fe^{3+}, and the rate data are correlated by the semiempirical expression $\ln [(N_2H_4)/(N_2H_4)_0] = -[a'(Fe^{3+}) + b'(Fe^{2+})](H^+)t$ where $a' = 0.114$ M^{-2} min^{-1} and $b' = 0.065$ M^{-2} min^{-1}. A reaction mechanism is proposed for the ferric-catalyzed reaction whose major reactions involve the reduction of Fe^{3+} to Fe^{2+} by hydrazine and the oxidation of Fe^{2+} to Fe^{3+} by nitric acid.

Introduction

Hydrazine is used in nuclear fuel reprocessing as both a reducing agent and a nitrous acid scavenger.[1,2] As a reducing agent, hydrazine normally reacts slowly at room temperature but has reaction rates at higher temperatures rapid enough to be useful for the reduction of Pu(IV) and Np(V).[3] The rapid reaction of hydrazine with HNO_2 is applied to the stabilization of U(IV) nitrate, ferrous sulfamate, and hydroxylamine solutions in solvent-extraction and ion-exchange processes for the separation of uranium, actinides, and fission products. A recent application is the use of hydrazinium nitrate–HNO_3–KF solutions for dissolving plutonium metal.[4] Hydrazine prevents the precipitation of plutonium(IV) oxides during the dissolving of plutonium metal.

Many of these applications involve temperature and acid concentrations where the stability of hydrazine is unknown and where the maintenance of a hydrazine concentration is critical to the success of the process. This study was begun to provide more detailed information on the reaction rates and products of the hydrazine–nitric acid reaction. Since Fe(II) is used as a reagent in the chemical processing, the effect of Fe(II) and Fe(III) on hydrazine oxidation was also investigated.

Experimental Section

Reagents. Hydrazinium nitrate solution was purchased by the Savannah River Plant (SRP) from Fairmont Chemical Co., Newark, NJ, as a 3.6 M solution. The solution for the study was obtained from the plant stock. Nitric acid, sodium azide, sodium hydroxide, and ferric nitrate were CP grade reagents. Ferrous nitrate solution was prepared by dissolving iron metal in 3 M HNO_3–0.5 M $N_2H_4 \cdot HNO_3$ at a temperature below 50 °C.

Analyses. Hydrazine was determined by the indirect iodate method. The sample was added to a measured excess of standard KIO_3 solution, acidified with 2 M H_2SO_4, and mixed for 1 min or more. Unreacted KIO_3 was reduced to I_2 with an excess of 0.1 M KI solution, and liberated I_2 was titrated with standard $Na_2S_2O_3$ solution.

Hydrazoic acid was determined by two methods. For small samples, the solution was mixed with HNO_3–$Fe(NO_3)_3$ solution and the concentration of the FeN_3^{2+} complex determined spectrophotometrically.[5] When large amounts of sample (~5 mL) were available, HN_3 was nitrogen-sparged from an acid solution and collected by absorbing the vapor in a measured volume of standard NaOH solution. A few drops of $Fe(NO_3)_3$ solution were added to the sample before sparging; the disappearance of the red-brown FeN_3^{2+} color indicated complete removal of HN_3. Hydrazoic acid was then determined by titration with standard Ce^{4+}.[6]

Nitric acid was determined by titration with standard base with a methyl red indicator. Ammonium ion was determined with an ammonia electrode (Orion Associates, Cambridge, MA).

Gas samples were analyzed by a Hewlett-Packard Model 5750 gas chromatograph with a Carbosieve column. Results were corrected for air leakage from oxygen analyses.

Ferrous ion was determined by titration with standard ceric sulfate solution in 2 M H_2SO_4. Tests found that interference from HN_3 or N_2H_4 was negligible under these conditions.

Procedure. The reaction vessel was a two-necked 100-mL flask immersed in a thermostated oil bath. One neck of the flask was used for reagent addition and liquid sampling; the other neck was fitted with a reflux condenser that was connected at its upper end to a gas sample bulb. The gas sample bulb was in turn connected to a water-filled flask. Evolution of gas during the reaction displaced water into a graduated cylinder for measurement. The reaction mixture was magnetically stirred. Gas volumes were determined in parallel experiments that were not disturbed by solution sampling.

The initial solution volume in all experiments was 52 mL. Eighteen milliliters of concentrated nitric acid (15.7 M) and a combined volume of 26 mL of water, 10 M NaOH, and 1.3 M $Fe(NO_3)_3$ solution were mixed and brought to the selected temperature in the oil bath; the reaction was initiated by adding 8 mL of 3.6 M $N_2H_4 \cdot HNO_3$ solution. NaN_3 and $Fe(NO_3)_2$ were added after the hydrazine addition in experiments where their effects on the reaction were explored. The initial ionic strength ($HNO_3 + NaNO_3 + N_2H_4 \cdot HNO_3$) was 6.0 M; the final ionic strength ($HNO_3 + NaNO_3 + HN_3 + NH_4NO_3$) was ~5.6–5.8 M.

The concentration of $NaNO_3$ in this study is always the difference between 5.44 M and the acid concentration. For example, a reaction in 4.41 M HNO_3 in this paper is a reaction in 4.41 M HNO_3–1.03 M $NaNO_3$.

Results

A. Nitric Acid Oxidation of Hydrazine. Acid Dependence. Experiments in 6.0 M NO_3^- at 100 °C established initially that the reaction was first order in hydrazine. Figure 1 shows a typical first-order plot for the concentration of hydrazine with time for the initial conditions 4.38 M HNO_3–0.55 M $N_2H_4 \cdot HNO_3$. The reaction rate was also found to depend on the square of the acidity (Table I).

Reaction Products. The products of the hydrazine–HNO_3 reaction are N_2, N_2O, HN_3, and NH_4^+; no NO or NO_2 was detected in any of the gas samples. Figure 2 shows the concentrations of N_2H_4, NH_4^+, and HN_3 during the reaction and the rate of gas evolution during the reaction in 5.44 M HNO_3 at 100 °C. The decrease in HN_3 concentration near the end of the reaction indicates that HN_3 is being destroyed as well as produced in the system. A 1-h test in 6 M HNO_3 at 100 °C found that there was no change in the concentration of NH_4^+ within the limits of error of the experiment, ±3%. Ammonium ion is therefore considered to be a final product. Data for the solution products of the reaction are presented in Table I.

HN_3 Volatility. Pure HN_3 is quite volatile (bp 37 °C)[7] and is easily removed from acid solutions by a sparging gas stream.[8-10]

† The information contained in this article was developed during the course of work under Contract No. DE-AC09-76SR00001 with the U.S. Department of Energy.

(1) Kelmers, A. D.; Valentine, D. Y. "Search for Alternate Holding Reductants to Stabilize Plutonium(III) Solutions", Report ORNL/TM 6521; Oak Ridge National Laboratory: Oak Ridge, TN, Sept 1978.
(2) Perrott, J. R.; Stedman, G. *J. Inorg. Nucl. Chem.* **1977**, *39*, 325.
(3) Karraker, D. G. "Hydrazine Reduction of Np(V) and Pu(IV)", USDOE Report DP-1601; E. I. du Pont de Nemours & Co., Savannah River Laboratory: Aiken, SC, Nov 1981.
(4) Karraker, D. G. "Dissolution of Plutonium Metal in HNO_3–N_2H_4–KF", USDOE Report DP-1666; E. I. du Pont de Nemours & Co., Savannah River Laboratory: Aiken, SC, July 1983.
(5) Dukes, E. K.; Wallace, R. M. *Anal. Chem.* **1961**, *33*, 42.
(6) Arnold, J. M. *Ind. Eng. Chem., Anal. Ed.* **1945**, *17*, 215.
(7) Yost, D. M.; Russell, H., Jr. "Systematic Inorganic Chemistry"; Prentice-Hall: New York, 1946; p 119.
(8) Maya, B. M.; Stedman, G. *J. Chem. Soc., Dalton Trans.* **1983**, 257.
(9) Templeton, J. C.; King, E. L. *J. Am. Chem. Soc.* **1971**, *93*, 7160.

0020-1669/85/1324-4470$01.50/0

Table I. Reaction Data for N_2H_4 Oxidation at 100 °C[a]

	final concn, M					
(HNO_3), M	N_2H_4	HN_3	NH_4^+	reacn half-time, h	half-time × $(HNO_3)^2$	10^5k,[b] M^{-3} min^{-1}
5.44	0.083	0.077	0.061	1.08	32.0	6.00
5.20	0.035	0.078	*c*	1.2	32.4	5.96
5.05	0.041	0.030	0.085	1.4	35.7	5.41
4.41	0.12	0.096	0.067	1.6	31.1	6.21
3.90	0.074	0.072	0.063	2.1	31.9	6.05
3.41	0.22	0.13	0.062	3.0	34.9	5.53
3.04	0.18	0.090	0.070	3.3	29.7	6.49
2.98	0.19	0.095	*c*	3.9	34.6	5.58
2.56	0.33	0.077	0.055	5.5	36.0	5.36
					33.2 ± 1.9 (av)	5.83 ± 0.33 (av)

[a] Initial conditions: 0.55 M $N_2H_4 \cdot HNO_3$, μ = 6.0. [b] k for d ln $(N_2H_4)/dt = k(NO_3^-)(H^+)^2$. [c] Not determined.

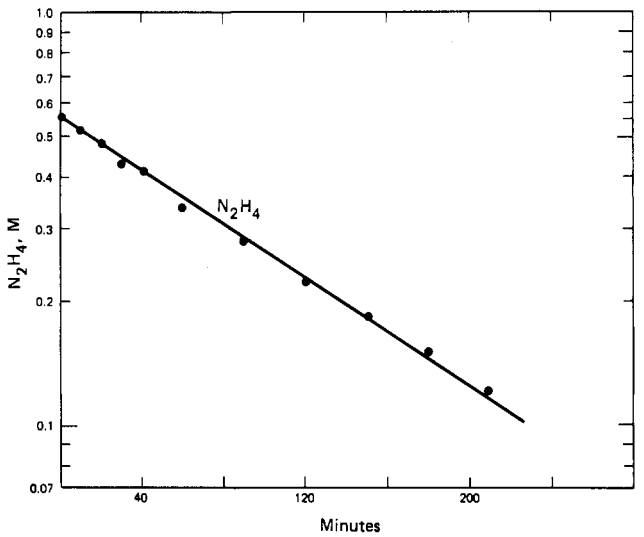

Figure 1. Typical rate data. Reaction conditions: 4.38 M HNO_3, 1.24 M $NaNO_3$, 100 °C.

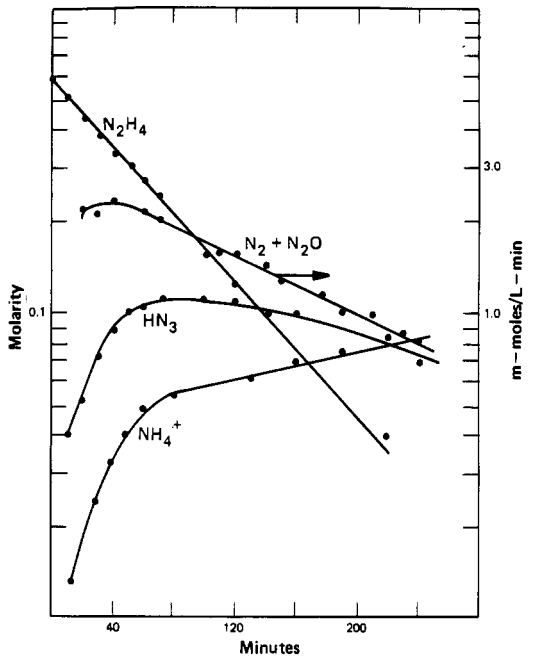

Figure 2. Concentration of reaction products in 5.44 M HNO_3 at 100 °C.

However, no HN_3 could be detected escaping the condenser in these experiments. Tests of the stability of HN_3 in 5.4 M HNO_3 found a 2.4% loss in 1 h at 80 °C and a 20% loss in 1 h at 100 °C. The loss at 100 °C is believed due to the oxidation of HN_3 by HNO_3, and a calculated first-order rate constant for this loss is ca. 4×10^{-3} min^{-1}. Other workers have reported a first-order rate constant of 5.1×10^{-3} min^{-1} at 97 °C for the oxidation of HN_3 by 6.1 M HNO_3.[8] The HN_3–HNO_3 reaction rate is strongly acid-dependent,[8] so the agreement between values is quite good and supports the assumption that oxidation by HNO_3 is responsible for HN_3 loss at 100 °C.

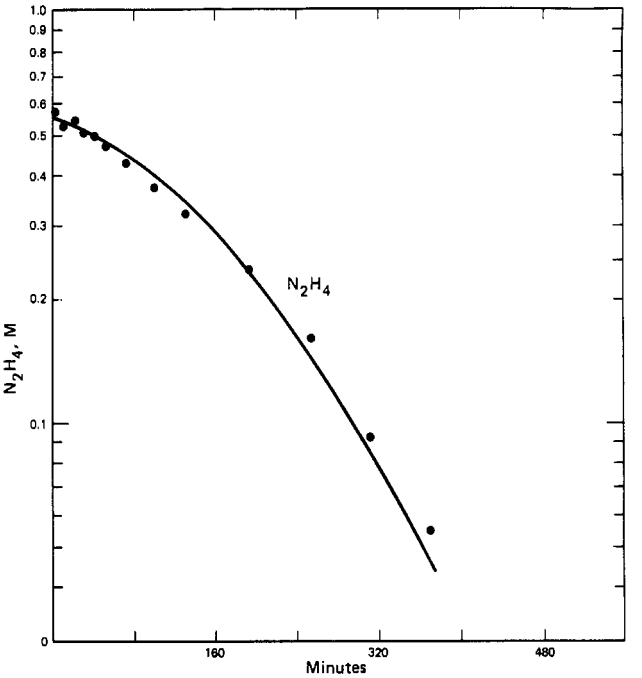

Figure 3. Data for the N_2-sparged reaction for 4.35 M HNO_3–1.22 M $NaNO_3$ at 100 °C and 70 mL of N_2/min.

In several experiments, HN_3 was continuously removed from solution by a sparging nitrogen stream and collected from the N_2 stream by scrubbing with 0.1 M NaOH. The effect of HN_3 removal on the oxidation of N_2H_4 is shown in Figure 3; the continuous removal of HN_3 causes a deviation from a first-order reaction. The HN_3 recovered in the NaOH-filled scrubber corresponded to a 90% yield for HN_3 from N_2H_4–nitrogen. Sparging the solution is a simple preparation for HN_3 or NaN_3.

The oxidation of hydrazine can be expected to have a free-radical mechanism.[11-13] Several attempts were made to scavenge free radicals by sparging the reacting solution with ethylene or acetylene at flow rates up to 70 mL/min. The rate data were indistinguishable from data obtained by N_2 sparging, so it was concluded that the experiments were unsuccessful. Neither C_2H_4 or C_2H_2 is a particularly good radical scavenger, but normal radical scavengers are too unstable for use in this system.

Gaseous Products. After a brief induction period, N_2 and N_2O are evolved at a rate that decreases more slowly than the decrease

(10) D'Orazio, L. A.; Wood, R. H. *J. Phys. Chem.* **1963**, *67*, 1435.
(11) Higginson, W. C. E. *Spec. Publ.—Chem. Soc.* **1957**, *No. 10*, 95–112.
(12) Cahn, J. W.; Powell, R. E. *J. Am. Chem. Soc.* **1954**, *76*, 2568.
(13) Higginson, W. C. E.; Wright, P. *J. Chem. Soc.* **1955**, 1551.

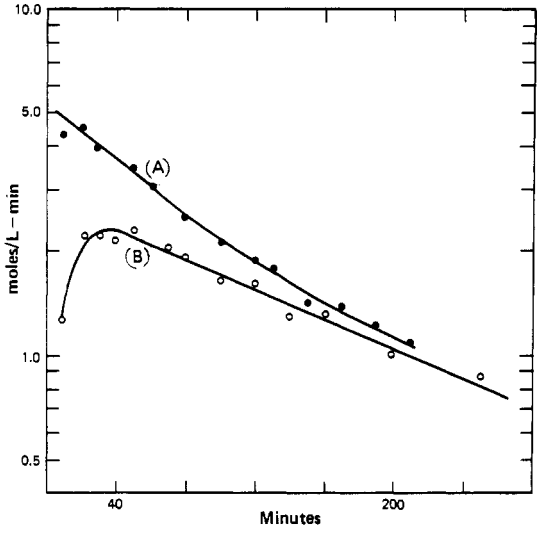

Figure 4. Gas evolution rates at 100 °C for (A) 5.44 M HNO_3–0.55 M N_2H_4·HNO_3–0.15 M NaN_3 and (B) 5.44 M HNO_3–0.55 M N_2H_4·HNO_3.

Table II. Gas Evolution Data[a] at 100 °C

			vol %	
(HNO_3), M	(NaN_3), M	gas yield, mmol	N_2	N_2O
5.5		22.3	76	24
4.0		17.3	77	23
3.0		10.6	79	21
5.5	0.15	30.6	72	28
3.0	0.15	11.1	73	27

[a] Initial (N_2H_4·HNO_3) was 0.55 M.

in N_2H_4 concentration (Figure 4). The gas evolved is 21–24% N_2O, and the N_2O content does not appear to be significantly affected by acidity (Table II). The initial addition of HN_3 leads to a rapid initial evolution of gas that is richer in N_2O than normal and to an increase in the total gas evolved (Table II, Figure 4). A simple calculation indicates that about 40% of the gas evolved from the HN_3 addition is N_2O, suggesting that the reaction

$$HN_3 + HNO_2 \rightarrow N_2 + N_2O + H_2O$$

is a major contributor to the production of N_2O.

Temperature Effects. The oxidation of hydrazine by nitric acid has a strong temperature dependence. Reaction half-times in 5.44 M HNO_3 at lower temperatures (h, °C): 2.7, 90; 8, 80; 33, 70. The corresponding values for k are shown graphically vs. $1/K$ in Figure 5. The constants for the Arrhenius equation

$$k = A \exp(-E/RT)$$

are $A = 1.2 \times 10^{11}$ M^{-3} min^{-1} and $E = 26$ kcal/mol.

Net Reaction. The net reaction depends on the time allowed for the reaction. For a reaction in 5.44 M HNO_3 at 100 °C that was 75% complete, the net reaction is approximately

$$N_2H_4 + 0.8HNO_3 \rightarrow$$
$$0.19HN_3 + 0.17NH_4NO_3 + 0.7N_2 + 0.2N_2O + 1.8H_2O$$

B. Iron-Catalyzed Oxidation of Hydrazine. Nature of the Reaction. The catalytic effect of iron ions was studied primarily at 80 °C and with an initial iron concentration of 0.1 M. These conditions were chosen to keep the reaction rate in a measurable range for the sampling techniques used, to have iron concentrations in a measurable range by titration techniques, and to ensure that the main route of the hydrazine oxidation would be by the iron-catalyzed reaction, rather than nitric acid oxidation. Preliminary experiments found reaction half-times of 0.33, 2.7, and 8 h for 0.1 M, 10^{-2} M, and zero ferric nitrate, respectively, added initially to the reaction mixture. From these data, it can be calculated that 97% of the hydrazine oxidation occurs by the iron-catalyzed route at 80 °C with 0.1 M $Fe(NO_3)_3$ initially present, but only

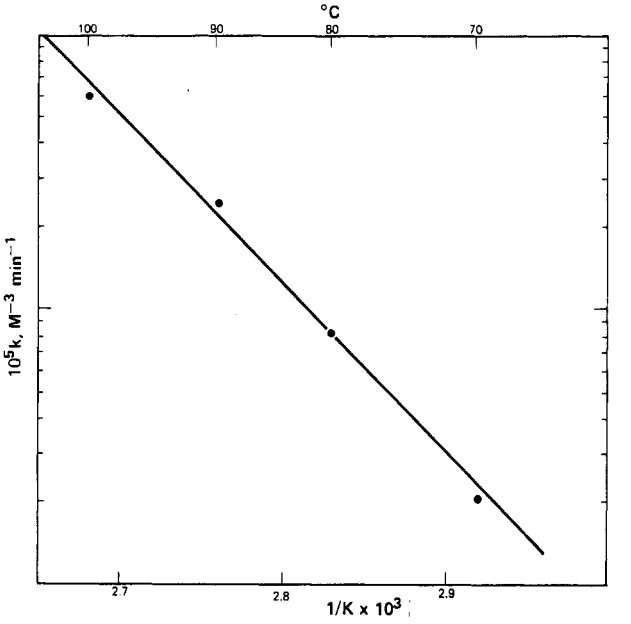

Figure 5. Temperature dependence of the reaction in 5.44 M HNO_3.

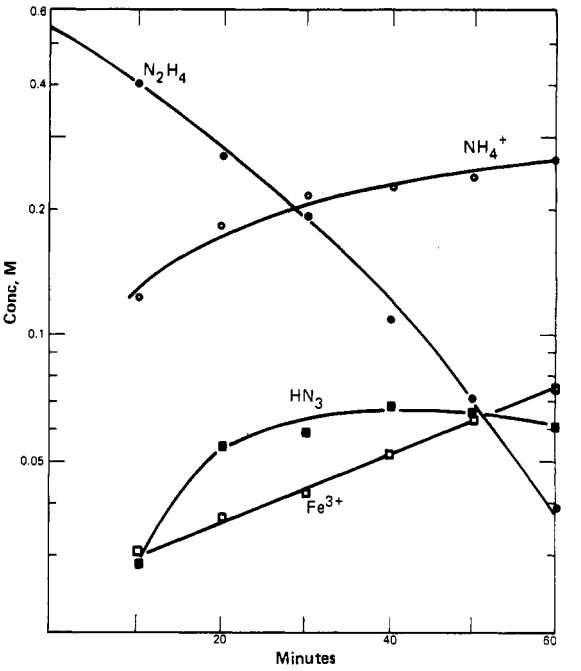

Figure 6. Reactant concentrations. Initial conditions: 4.67 M HNO_3, 0.1 M $Fe(NO_3)_3$, 0.55 M N_2H_4·HNO_3, 80 °C.

55% of the oxidation proceeds through a catalytic path when the initial $Fe(NO_3)_3$ concentration is 10^{-2} M.

Preliminary experiments found that not only were the iron ions oxidized and reduced during the reaction but also the first-order oxidation of hydrazine accelerated as the ferric concentration increased (Figure 6). Iron ions were added both as $Fe(NO_3)_3$ and as hydrazine-stabilized $Fe(NO_3)_2$. When 0.1 M Fe^{3+} was added initially, there was a rapid evolution of gas during the first 10 min of the reaction at 80 °C in 2.93 M HNO_3, but when the initial iron addition was 0.1 M Fe^{2+}, there was only a minor gas evolution (Figure 7). The measured difference between initial additions of Fe^{3+} and Fe^{2+} was 2.3 mmol of gas. This initial reaction was expected from the results of earlier investigators[11-13] and is due to

$$N_2H_5^+ + Fe^{3+} \rightarrow N_2H_3 + Fe^{2+} + 2H^+$$

followed by

$$2N_2H_3 + 2H^+ \rightarrow 2NH_4^+ + N_2$$

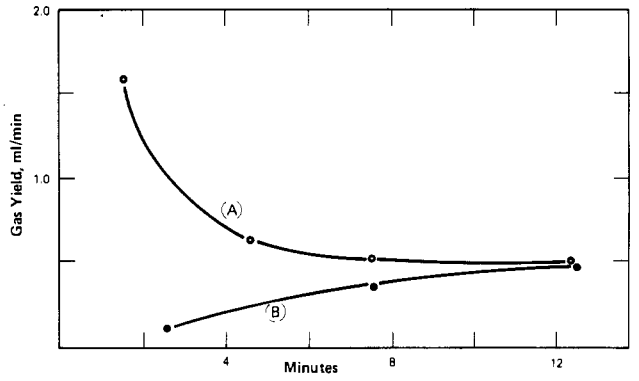

Figure 7. Gas evolution from 2.93 M HNO_3–0.55 M N_2H_4·HNO_3 at 80 °C with an initial addition of (A) 0.1 M $Fe(NO_3)_3$ or (B) 0.1 M $Fe(NO_3)_2$.

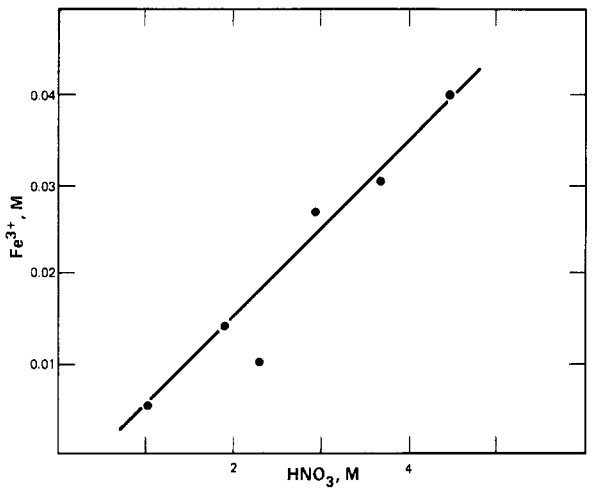

Figure 8. Fe^{3+} concentration 10 min after reaction initiation.

Table III. Initial Fe^{3+} Concentration[a] and Reaction Half-Times

(HNO_3), M	T, °C	(Fe^{3+}), M	reacn half-time, min
5.44	80	0.040	16
4.67	80	0.030	18
3.90	80	0.027	22
3.30	80	0.010	26
2.93	80	0.014	28
1.99	80	0.005	48
5.44	70	0.038	60
3.90	70	0.039	62
3.90	90	0.039	14
2.93	90	0.01	9
5.44[b]	90	c	33
3.90[b]	90	c	84

[a] Initial concentrations: 0.55 M N_2H_4·HNO_3, (Fe^{3+}) + (Fe^{2+}) = 0.1 M. [b] (Fe^{3+}) + (Fe^{2+}) = 0.013 M. [c] Not determined.

The reduction of the 5.2 mmol of Fe^{3+} initially added could produce 2.6 mmol of N_2. As the reduction of Fe^{3+} in the first 10 min is 87% complete, the expected yield of N_2 is 2.26 mmol. The 2.3-mmol experimental value agrees well with the calculated value.

The initial reduction of Fe^{3+} depends on both the acid concentration and the temperature. Higher acidities and higher temperatures result in a higher Fe^{3+} concentration in the initial stage of the reaction. The concentration of Fe^{3+} 10 min after reaction initiation at varying acidities is shown in Figure 8; data on Fe^{3+} concentration and initial reaction half-times are shown in Table III.

The Fe^{3+} concentration measured 10 min after the start of the reaction is normally the minimum concentration and increases during the hydrazine oxidation. The Fe^{3+}/Fe^{2+} ratio maintains a steady state between the reduction of Fe^{3+} by hydrazine and reducing intermediates and the oxidation of Fe^{2+} by HNO_3. When the hydrazine concentration becomes small, the Fe^{3+} concentration increases and the reaction rate increases, as in Figure 6.

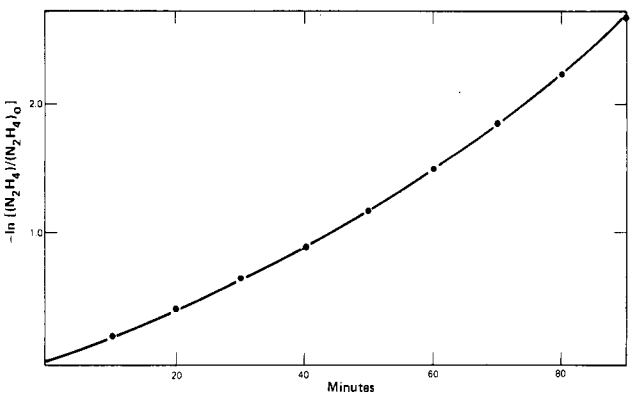

Figure 9. Data fit for 2.93 M HNO_3–0.1 M $Fe(NO_3)_3$–0.55 M N_2H_4·HNO_3 at 80 °C. Points are experimental; line is a computer fit.

Table IV. Least-Squares Constants from Data Fit[a]

(HNO_3), M	T, °C	a, M^{-1} min^{-1}	$a/(H^+)$	b, M^{-1} min^{-1}	$b/(H^+)$
5.44	80	0.656 ± 0.029	0.121	0.348 ± 0.055	0.064
4.67	80	0.448 ± 0.012	0.096	0.311 ± 0.026	0.066
3.90	80	0.414 ± 0.008	0.106	0.239 ± 0.010	0.061
3.30	80	0.416 ± 0.017	0.125	0.243 ± 0.017	0.073
2.93	80	0.364 ± 0.004	0.124	0.184 ± 0.004	0.063
1.99	80	0.402 ± 0.015	0.201	0.176 ± 0.003	0.086
5.44	70	0.180 ± 0.005	0.033	0.098 ± 0.008	0.018
3.90	90	1.02 ± 0.05	0.262	0.98 ± 0.14	0.025
3.90	70	0.147 ± 0.002	0.038	0.073 ± 0.003	0.019

[a] Initial conditions: 0.55 M N_2H_4·HNO_3, 0.10 M Fe^{3+}, μ = 6.3. Constants for $-\ln [(N_2H_4)/(N_2H_4)_0] = [a(Fe^{3+}) + b(Fe^{2+})]t$.

Reaction Rates. Table III shows the reaction half-times as measured by the initial slope of a graph like Figure 6. Between 5.44 and 2.93 M HNO_3 at 80 °C, the reaction has a first-power dependence on acidity. The reaction rate increases about a factor of 3 for each 10 °C increase in the temperature.

A more detailed analysis of the data involved a computer fit of the data to a two-path model. Of the several fits attempted, the best fit was achieved for the model

$$-\ln [(N_2H_4)/(N_2H_4)_0] = [a(Fe^{3+}) + b(Fe^{2+})]t$$

where $(N_2H_4)_0$ is the initial concentration of hydrazine and the values for (N_2H_4), (Fe^{3+}), and (Fe^{2+}) are the experimental values measured at time t (min).

The run data were fit with a nonlinear least-squares program (PROC NLIN) in the SAS[14] system on an IBM 3081 computer to determine values for the coefficients a and b. A sample of the computer fit for one data set (2.93 M HNO_3, 0.1 M $Fe(NO_3)_3$, 0.55 M N_2H_4·HNO_3, 80 °C, initial conditions) is shown in Figure 9. The average deviation for this data set between the experimental data and the computer fit was 1.4%. Values for a and b for all data are shown in Table IV.

The values for both a and b show a linear dependence on acidity for the data at 80 °C at 2.93 M HNO_3 and higher acidities. (See the first five entries in columns 4 and 6, Table IV.) At 80 °C, $a = 0.114(H^+)$ and $b = 0.065(H^+)$; the computer-fitted data can be represented empirically by

$$-\ln [(N_2H_4)/(N_2H_4)_0] = [0.114(H^+)(Fe^{3+}) + 0.065(H^+)(Fe^{2+})]t$$

where t is in minutes.

Temperature Dependence. The temperature dependence of $a' = a/(H^+)$ and $b' = b/(H^+)$ was determined from a graph of the appropriate values from Table IV vs. $1/T$ (Figure 10). The

(14) SAS Institute, Inc., P.O. Box 8000, Cary, NC 25711.

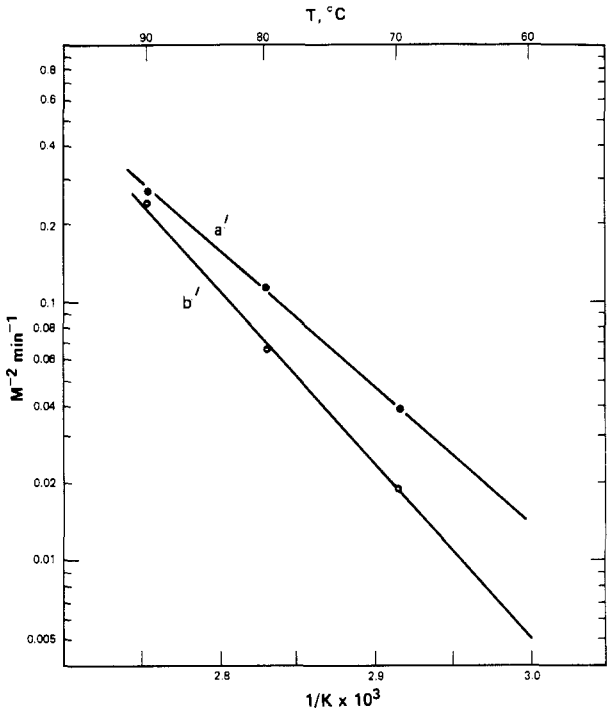

Figure 10. Temperature dependence of constants a' and b'.

Table V. Reaction Products for Fe^{3+}/Fe^{2+}-Catalyzed Hydrazine Oxidation

initial			final				
			mmol			%	
(HNO_3), M	(Fe^{3+}), M	T, °C	NH_4^+	HN_3	$N_2 + N_2O$	N_2	N_2O
5.44	0.1	90	16.1	2.6	20.9	76	23
	0.1	80	16.6	2.5	19.0	79	21
		90	4.7	4.9		74	26
	0.013[a]	90	13.0	3.2	20.4		
	0.076[a]	65	14.0	3.6	13.7[b]	82	18
	0.013	90	13.5	3.2	18.5	69	31
4.67	0.1	80	15.1	2.9	19.3	72	28
3.90	0.1	90	14.0	2.0		80	20
	0.1	80	16.6		19.9	72	28
	0.01	90	16.6	3.1			
	0.1	70					
2.93	0.1	80	12.5	3.6		71	29
1.99	0.1	80	15.1	3.1	19.3	68	32

[a] Fe^{2+}. [b] Reaction incomplete.

temperature dependence of b' is about 30% greater than the temperature dependence of a'.

Reaction Products. The reaction products (Table V) show remarkably little variation with temperature and acidity. There is a slight increase in the N_2O yield at lower acidity that may be real. However, the percentages of N_2 and N_2O change enough during a reaction that the composition of the gas sample can be affected by the time of sampling. In a reaction at 90 °C, 5.44 M HNO_3, and 0.10 M $Fe(NO_3)_3$, gas samples showed 89%, 74%, and 65% N_2 at the beginning, middle, and end of the reaction, respectively. Large gas samples were taken to obtain an average value, but the gas samples did not include all the gas produced during a reaction.

The major difference between the Fe^{3+}-catalyzed and the uncatalyzed reaction is the large increase in NH_4^+ produced in the catalyzed reaction. The uncatalyzed reaction (Figure 2) produces roughly equal amounts of NH_4^+ and HN_3; the Fe^{3+}-catalyzed reaction produces about 5 times as much NH_4^+ as HN_3.

Net Reaction. The net reaction at 80 °C in 2.93 M HNO_3 with 0.1 M Fe^{3+} catalyst can be calculated from the data of Table V to be

$$N_2H_4 + 1.4HNO_3 \rightarrow 0.56N_2 + 0.24N_2O + 0.15HN_3 + 0.70NH_4NO_3 + 1.5H_2O$$

Discussion

A. Hydrazine Oxidation by Nitric Acid. Reaction Mechanism. The mechanisms for the oxidation of hydrazine have been the subject of kinetic investigation for over 60 years, but no study of the oxidation of hydrazine by nitric acid has been reported. (Stedman and co-workers[8] indicate that they have a study in progress.) Hydrazine can react with one-electron-oxidizing agents (Fe^{3+}) to produce the hydrazyl radical, N_2H_3, or with two-electron-oxidizing agents (HNO_3) to produce the diazene radical, N_2H_2.[11-13] If one accepts the proposal[11] that the initial step is the formation of HNO_2 and the diazene radical, the initial reaction is

$$N_2H_5^+ + HNO_3 \xrightarrow{k_1} N_2H_2 + H^+ + HNO_2 + H_2O \quad (1)$$

followed by the very rapid[1,2] reaction between $N_2H_5^+$ and HNO_2

$$N_2H_5^+ + HNO_2 \xrightarrow{k_2} HN_3 + 2H_2O + H^+ \quad (2)$$

The reactions with initial additions of NaN_3 showed both increased N_2–N_2O yields and an increase in the N_2O/N_2 ratio. This suggests the secondary reaction[15]

$$HN_3 + HNO_2 \xrightarrow{k_3} N_2 + N_2O + H_2O \quad (3)$$

The N_2H_2 radical reaches a steady state between its formation in reaction 1 and its destruction by

$$N_2H_2 + HN_3 + H^+ \xrightarrow{k_4} 2N_2 + NH_4^+ \quad (4)$$

$$N_2H_2 + HNO_3 \xrightarrow{k_5} N_2 + HNO_2 + H_2O \quad (5)$$

HN_3 also reaches a steady state among reactions 2–4. These reactions were found sufficient to derive rate laws for each of the reaction products that were consistent with the experimental data.

Other reactions were considered but ruled out as inconsistent with the experimental data or unlikely from reactant concentrations. The reaction[8] between HN_3 and HNO_3 yields a mixture of N_2, N_2O, and NO as gaseous products and was not considered, since no NO was found in analyses of the product gases. The radical–radical dis- and reapportionation reactions of N_2H_2 have been suggested[11]

$$H^+ + 2N_2H_2 \rightarrow N_2 + N_2H_5^+$$

$$H^+ + 2N_2H_2 \rightarrow HN_3 + NH_4^+$$

but require reactions between two N_2H_2 radicals, which must be present in very low concentration. A reaction between two N_2H_2 radicals is therefore unlikely to be a major reaction in this system. The reaction

$$N_2H_2 + HNO_3 \rightarrow {}^3/_2N_2O + {}^3/_2H_2O$$

appears plausible, but on detailed analysis leads to N_2O/N_2 ratios greater than 1, in disagreement with the experimental data.

To describe the system conceptually, as hydrazine is oxidized, the reactive species HNO_2, N_2H_2, and HN_3 are produced and achieve a steady state between their production and destruction. When steady-state conditions are established, the oxidation proceeds by a first-order rate law.

Rate Laws. From the equilibria described by

$$K_1 = \frac{(N_2H_5^+)}{(N_2H_4)(H^+)} \approx 8.5 \times 10^7 \text{ at } 25\ ^\circ\text{C}^7 \quad (6)$$

$$K_2 = \frac{(HNO_3)}{(NO_3^-)(H^+)} \approx 22 \text{ at } 25\ ^\circ\text{C}^{14} \quad (7)$$

and reaction 1, the experimental rate law is derived as

$$d(N_2H_4)/dt = -k_1(N_2H_5^+)(HNO_3) \quad (8)$$

$$d(N_2H_4)/dt = -k_1K_1K_2(N_2H_4)(NO_3^-)(H^+)^2 \quad (9)$$

(15) Phelan, K. G.; Stedman, G. *J. Chem. Soc., Dalton Trans.* **1982**, 1603.

or

$$\mathrm{d} \ln (N_2H_4)/\mathrm{d}t = -k'(NO_3^-)(H^+)^2 = -F \quad (10)$$

$$k' = k_1K_1K_2 \qquad F = k'(NO_3^-)(H^+)^2$$

This corresponds to the experimental rate law.

Rate laws for the concentration with time of N_2H_4, NH_4^+, and HN_3 are derived in the Appendix from reactions 1–5. The derivations assume steady-state concentrations for N_2H_2 and HNO_2, omit terms of lesser magnitude, and treat some slowly varying terms as constants. The derived rate laws will be compared with the data sets for the acid range 3–5.44 M and illustrated for data at 5.44 M (Figure 2 and Table VI).

$$\ln \frac{(N_2H_4)}{(N_2H_4)_0} = -nFt \quad (11)$$

$$n = \frac{2k_4(HN_3) + 3k_5'(NO_3^-)}{k_4(HN_3) + k_5'(NO_3)}$$

The value of n, considering HN_3 as a constant, was obtained by comparing rate data for NH_4^+ with the rate law for NH_4^+ derived in the Appendix. The rate law for NH_4^+ is

$$(NH_4^+) = \frac{k_4(HN_3)[(N_2H_4)_0 - (N_2H_4)_t]}{2k_4(HN_3) + 3k_5'(NO_3^-)} \quad (12)$$

A graph (Figure 11) of (NH_4^+) vs. $[(N_2H_4)_0 - (N_2H_4)_t]$ for the data of Figure 2 (tabulated in Table VI) shows a linear fit to the experimental data.

The slope of the straight line (Figure 11) had an average value of 0.155 ± 0.010 for four sets of data over the acid range 3–5.44 M. Then

$$0.155 = \frac{k_4(HN_3)}{2k_4(HN_3) + 3k_5'(NO_3^-)} \quad (13)$$

from which $k_4(HN_3)/k_5'(NO_3^-) = 0.67$ and $n = 2.60$. The experimental first-order rate constant $k = nk' = 5.83 \times 10^{-5}$ M^{-3} min^{-1}; hence, $k' = k_1K_1K_2 = 2.24 \times 10^{-5}$ M^{-3} min^{-1}.

The rate law for HN_3 as derived in the Appendix is

$$(HN_3) = \frac{[1 - k_4(HN_3)][(N_2H_4)_0 - (N_2H_4)_t]}{2k_4(HN_3) + 3k_5'(NO_3^-)} - \frac{Fk_3(HN_3)[1 + k_4(HN_3)]}{k_2'(H^+)[k_4(HN_3) + k_5'(NO_3^-)]}t \quad (14)$$

Figure 12 shows data from Table VI graphed against $[(N_2H_4)_0 - (N_2H_4)_t]$. The initial slope of the graph is due to the first term in eq 14, and the curvature at high values is approximated by the second term. Three other sets of data over the acid range 3–5.5 M HNO_3 had an initial slope of 0.48 ± 0.01, with no apparent trend with acid concentration. A least-squares program fitted the data of Table VI to eq 14 (Figure 12), yielding

$$\frac{1 - k_4(HN_3)}{2k_4(HN_3) + 3k_5'(NO_3^-)} = 0.482 \pm 0.015 \quad (15)$$

and

$$\frac{Fk_3(HN_3)[1 + k_4(HN_3)]}{k_2'(H^+)[k_4(HN_3) + k_5'(NO_3^-)]} = 8.4\ (\pm 0.5) \times 10^{-4} \quad (16)$$

Equation 15 combined with the ratio $k_4(HN_3)/k_5'(NO_3^-) = 0.67$ from eq 13 yields $k_4(HN_3) = 0.25$ and $k_5'(NO_3^-) = 0.37$. From these values and eq 16, $k_2'(H^+)/k_3(HN_3) \cong 8$, which supports the assumption used for this approximation in the Appendix, eq A14.

An estimate of the concentration of the N_2H_2 free radical can be made from the rate law for nitrogen. This rate law

$$\mathrm{d}(N_2)/\mathrm{d}t = \mathrm{d}(N_2O)/\mathrm{d}t + [2k_4(HN_3) + k_5'(NO_3^-)](H^+)(N_2H_2) \quad (17)$$

can be solved for the N_2H_2 concentration from the values for

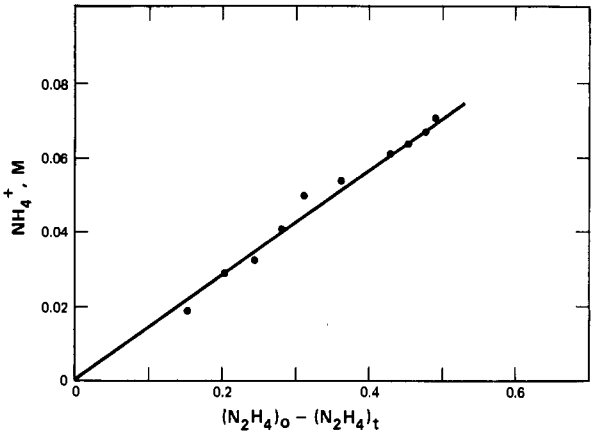

Figure 11. Test of eq 12 (data from Table VI for 5.44 M HNO_3 and 100 °C).

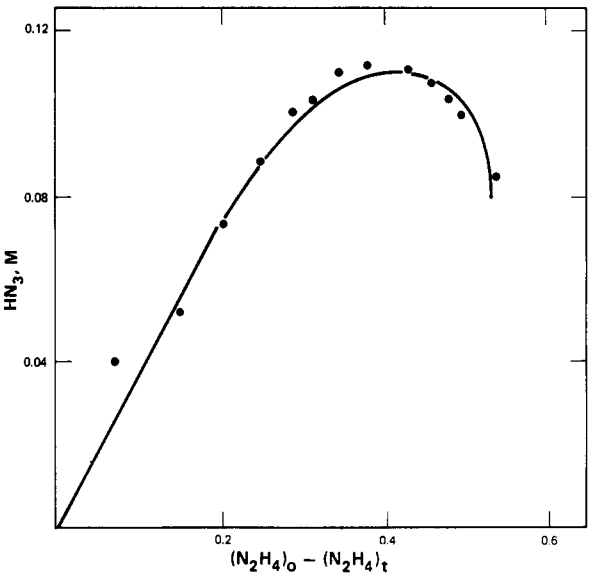

Figure 12. HN_3 data at 5.44 M HNO_3 and 100 °C. Points are data; line is calculated from (14).

$k_4(HN_3)$ and $k_5'(NO_3^-)$ and the data (Table VI) for the rate of N_2 and N_2O evolution (Appendix). When these values are substituted, N_2H_2 concentration is calculated to be $\sim 2 \times 10^{-4}$ M during the first reaction half-time. When average values for HN_3 and NO_3^- are substituted, $k_4 = 3.1$ M^{-3} min^{-1} and $k_5' = k_5K_2 = 0.062$ M^{-2} min^{-1}. As K_2 is of the order of 10, reaction 4 must be at least 100 times faster than reaction 5.

B. Ferric Catalysis. Reaction Mechanism. The proposed mechanism for the Fe^{3+}-catalyzed oxidation of hydrazine proceeds through the oxidation of hydrazine by Fe^{3+} and the oxidation of Fe^{2+} to Fe^{3+} by HNO_3. These reactions compete to create a steady-state concentration of Fe^{3+}, the primary oxidant for hydrazine. However, the detailed mechanism is considerably more complex. Hydrazine normally reacts with one-electron oxidants to form hydrazyl (N_2H_3) free radicals.[11,13,16] Reduction of HNO_3 can lead to NO_2, HNO_2, and NO as intermediates.[17-20] The reactions of the intermediates lead to the final products N_2, N_2O, NH_4^+, and HN_3.

A plausible reaction mechanism begins with the primary reaction between Fe^{3+} and $N_2H_5^+$:

$$Fe^{3+} + N_2H_5^+ \rightarrow Fe^{2+} + 2H^+ + N_2H_3 \quad (18)$$

(16) Higginson, W. C. E.; Sutton, D.; Wright, P. *J. Chem. Soc.* **1953**, 1380.
(17) Stedman, G. *Adv. Inorg. Chem. Radiochem.* **1979**, *22*, *113*.
(18) Epstein, I. R.; Kustin, K.; Warshaw, L. J. *J. Am. Chem. Soc.* **1980**, *102*, 3751.
(19) Orban, M.; Epstein, I. R. *J. Am. Chem. Soc.* **1982**, *104*, 5918.
(20) Kummer, J. T. *Inorg. Chim. Acta* **1983**, *76*, L291.

Fe^{2+} is oxidized by HNO_3, and under conditions where HNO_3 is in large excess, the most probable reaction is

$$Fe^{2+} + HNO_3 + H^+ \rightarrow Fe^{3+} + NO_2 + H_2O \quad (19)$$

NO_2 must reduce rapidly to HNO_2, since no NO_2 or NO was found in any gas sample. Two paths are possible, reduction by Fe^{2+} or by $N_2H_5^+$, as

$$Fe^{2+} + NO_2 + H^+ \rightarrow Fe^{3+} + HNO_2 \quad (20)$$

$$N_2H_5^+ + NO_2 \rightarrow HNO_2 + N_2H_3 + H^+ \quad (21)$$

HNO_2 is rapidly scavenged by $N_2H_5^+$ and HN_3:[1,15,21]

$$HNO_2 + N_2H_5^+ \rightarrow HN_3 + H^+ + 2H_2O \quad (22)$$

$$HN_3 + HNO_2 \rightarrow N_2O + N_2 + H_2O \quad (23)$$

The hydrazyl free radical reacts[11] by

$$2N_2H_3 + 2H^+ \rightarrow 2NH_4^+ + N_2 \quad (24)$$

$$N_2H_3 + 2H^+ + Fe^{2+} \rightarrow N_2H_5^+ + Fe^{3+} \quad (25)$$

$$N_2H_3 + Fe^{3+} \rightarrow N_2H_2 + Fe^{2+} + H^+ \quad (26)$$

The diazene free radical also reacts[11] by

$$N_2H_2 + HN_3 + H^+ \rightarrow 2N_2 + NH_4^+ \quad (27)$$

$$N_2H_2 + 2Fe^{3+} \rightarrow 2Fe^{2+} + 2H^+ + N_2 \quad (28)$$

The relative importance of reactions 18–28 can be estimated from the data of Tables III and IV. These reactions are largely responsible for maintaining the Fe^{3+}–Fe^{2+} steady state and oxidizing N_2H_4. Reaction 23 is the only reaction that produces N_2O and thus accounts for about 55% of the gaseous products. Reaction 24 is most important in the early part of the reaction. As the N_2H_4 concentration is depleted, the concentration of N_2H_3 radicals decreases and the bimolecular reaction becomes less probable. Reactions 26–28 become more important as the reaction nears completion.

Rate Law. Ideally, a rate law for the concentration of the reactants and the products as a function of time could be derived from a steady-state treatment of reactions 18–28. However, the system is quite complicated and a number of approximations and assumptions were necessary to solve the equations. The derived rate law should have a form similar to the experimental rate law

$$\ln [(N_2H_4)/(N_2H_4)_0] = -[a'(Fe^{3+}) + b'(Fe^{2+})](H^+)t \quad (29)$$

where $a' = a/(H^+)$ and $b' = b/(H^+)$.

With different approximations, three different rate laws for hydrazine were derived. All three had the same leading term as the experimental rate law, $-k_1'(Fe^{3+})(H^+)t$ ($k_1' = a' = 0.114\ M^{-2}\ min^{-1}$ at 80 °C), but none agreed with the acid dependence of the second term. Attempts to computer-fit data to the derived rate laws were unsuccessful.

Conclusion

The experimental data for the oxidation of hydrazine by nitric acid are remarkably consistent with the rate laws derived from a relatively simple set of reactions, a circumstance that may be fortuitous. A change in experimental conditions that increases the reaction rate (higher temperatures, higher acid concentrations) could make some of the reactions that were not considered in this analysis significant and render the approximations of the treatment presented here inadequate. At lower acid concentrations and lower acidities, this study is considered satisfactory and should provide a useful basis for more elaborate studies, such as ^{15}N experiments.

The rationalization of the data for the ferric-catalyzed hydrazine oxidation is considered only partially successful. There is probably some competition with the uncatalyzed reaction at low acidities, and the relative importance of the reactions proposed for this system changes during the course of an experiment. Under such circumstances, it is difficult to estimate whether the inadequacy of the derived rate to be consistent even with the oxidation of hydrazine is due to the complexity of the system, the inadequacy of the proposed mechanism, or the approximations applied to obtain a solution. However, the experimental data fit can be used to predict the behavior of hydrazine in plant operations and this work could be a useful starting point toward further studies.

(21) Perrott, J. R.; Stedman, G. *J. Inorg. Nucl. Chem.* **1977**, *39*, 325.

Table VI. Run Data for 5.5 M HNO_3 at 100 °C

time, min	(N_2H_4), M	(HN_3), M	(NH_4^+), M	amt of gas evolved, mmol/(L min)
0	0.586			
10	0.514	0.040		1.3
20	0.432	0.052	0.018	2.2
30	0.381	0.073	0.024	2.1
40	0.337	0.088	0.032	2.15
50	0.302	0.101	0.040	2.3
60	0.270	0.104	0.049	
70	0.243	0.111		2.05
80	0.218	0.110	0.053	1.9
100	0.154	0.111	0.060	1.65
120	0.124	0.108	0.063	1.6
140	0.104	0.101	0.067	1.3
160	0.091	0.100	0.070	1.3
220	0.040	0.085	0.077	0.95
280	0.017	0.063	0.084	0.7

Acknowledgment. The author is grateful to W. L. Frazier for gas analyses, to R. L. Postles for the versatile and useful PROC NLIN program, and to J. C. Shaw for his experimental assistance.

Appendix. Derivation of the Rate Laws for the N_2H_4–HNO_3 Reaction

The rate law for N_2H_4 from reactions 1 and 2 is given by

$$d(N_2H_4)/dt = -F(N_2H_4) - k_2K_1(N_2H_4)(H^+)(NO_3^-) \quad (A1)$$

where $F = k'(NO_3^-)(H^+)^2$.

The rate law for HNO_2 from reactions 1, 2, and 5 is

$$d(HNO_2)/dt = F(N_2H_4) - k_2'(N_2H_4)(H^+)(HNO_2) - k_3(HN_3)(HNO_2) + k_5'(NO_3^-)(H^+)(N_2H_2) \quad (A2)$$

where $k_2' = k_2K_1$ and $k_5' = k_5K_2$.

The rate law for N_2H_2 is

$$d(N_2H_2)/dt = F(N_2H_4) - [k_4(HN_3) + k_5'(NO_3^-)](H^+)(N_2H_2) \quad (A3)$$

Equations A2 and A3 can be solved for (HNO_2) and (N_2H_2) by assuming steady-state conditions, i.e., $d(HNO_2)/dt$ and $d(N_2H_2)/dt$ both equal to zero. Then

$$(N_2H_2) = \frac{F(N_2H_4)}{(H^+)[k_4(HN_3) + k_5'(NO_3^-)]} \quad (A4)$$

and

$$(HNO_2) = \left(\frac{k_4(HN_3) + 2k_5'(NO_3^-)}{k_4(HN_3) + k_5'(NO_3^-)}\right)\frac{F(N_2H_4)}{k_2'(N_2H_4)(H^+) + k_3(HN_3)} \quad (A5)$$

Substituting eq A4 and A5 into eq A1 and rearranging yield

$$d \ln (N_2H_4)/dt = -F\{1 + k_2'(N_2H_4)(H^+)[k_4(HN_3) + 2k_5'(NO_3^-)]/[k_2'(N_2H_4)(H^+) + k_3(HN_3)][k_4(HN_3) + k_5'(NO_3^-)]\} \quad (A6)$$

If it is assumed that $k_2'(N_2H_4)(H^+) >> k_3(HN_3)$ (an assumption defended in the Discussion), then

$$k_2'(N_2H_4)(H^+) + k_3(HN_3) \cong k_2'(N_2H_4)(H^+)$$

$$d \ln (N_2H_4)/dt = -F\left(\frac{2k_4(HN_3) + 3k_5'(NO_3^-)}{k_4(HN_3) + k_5'(NO_3^-)}\right) \quad (A7)$$

Equation A7 can be integrated by considering the HN_3 concentration constant. The result is

$$\ln \frac{(N_2H_4)}{(N_2H_4)_0} = -nFt \quad \text{(A8)}$$

where

$$n = \frac{2k_4(HN_3) + 3k_5'(NO_3^-)}{k_4(HN_3) + k_5'(NO_3^-)}$$

The rate law for NH_4^+ from reaction 4 is

$$d(NH_4^+)/dt = k_4(HN_3)(H^+)(N_2H_2) \quad \text{(A9)}$$

Substituting from eq A4 for (N_2H_2) gives

$$d(NH_4^+)/dt = \frac{k_4(HN_3)(N_2H_4)F}{k_4(HN_3) + k_5'(NO_3^-)} \quad \text{(A10)}$$

(N_2H_4) is replaced by $(N_2H_4)_0 \exp(-nFt)$, and the resulting expression is integrated. After evaluation of the integration constant, the result is

$$(NH_4^+) = \left(\frac{k_4(HN_3)}{2k_4(HN_3) + 3k_5'(NO_3^-)}\right)(N_2H_4)_0[1 - \exp(-nFt)] \quad \text{(A11)}$$

A more useful form is the equivalent expression

$$(NH_4^+) = \frac{k_4(NH_3)}{2k_4(HN_3) + 3k_5'(NO_3^-)}[(N_2H_4)_0 - (N_2H_4)_t] \quad \text{(A12)}$$

where $(N_2H_4)_t$ is the N_2H_4 concentration at time t.

The rate law for HN_3, derived from reactions 2–4, is

$$d(HN_3)/dt = [k_2'(N_2H_4)(H^+) - k_3(HN_3)](HNO_2) - k_4(HN_3)(H^+)(N_2H_2) \quad \text{(A13)}$$

After equivalent expressions are substituted for HNO_2 and N_2H_2, eq A15 becomes

$$d(HN_3)/dt = F(N_2H_4)\{([k_2'(N_2H_4)(H^+)][1 - k_4(HN_3)] - k_3(HN_3)[1 + k_4(HN_3)])/[k_2'(N_2H_4)(H^+) + k_3(HN_3)] \times [k_4(HN_3) + k_5'(NO_3^-)]\} \quad \text{(A14)}$$

The fraction enclosed in braces will be represented below as m. The fraction m includes terms depending on HN_3 and N_2H_4, which are mixed to the extent that the separation of variables does not appear possible. The approach taken was to assume

$$k_2'(N_2H_4)(H^+) >> k_3(HN_3)$$

in the denominator of m. This leads, after substitution of $(N_2H_4)_0[1 - \exp(-nFt)]$ for N_2H_4 and integration, to the expression

$$(HN_3) = \frac{[1 - k_4(HN_3)][(N_2H_4)_0 - (N_2H_4)_t]}{2k_4(HN_3) + 3k_5'(NO_3^-)} - \frac{Fk_3(HN_3)[1 + k_4(HN_3)]t}{k_2'(H^+)[k_4(HN_3) + k_5'(NO_3^-)]} \quad \text{(A15)}$$

In form, eq A15 is an exponential growth combined with a linear decay, although the data would be expected to have an exponential decay. However, eq A15 does fit the data fairly well.

The rate law for N_2 from reactions 3–5 is

$$d(N_2)/dt = k_3(HN_3)(HNO_2) + [2k_4(HN_3) + k_5'(NO_3^-)](H^+)(N_2H_2) \quad \text{(A16)}$$

Since the rate law for N_2O from reaction 3 is

$$d(N_2O)/dt = k_3(HN_3)(HNO_2) \quad \text{(A17)}$$

then

$$d(N_2)/dt = d(N_2O)/dt + [2k_4(HN_3) + k_5'(NO_3^-)](H^+)(N_2H_2) \quad \text{(A18)}$$

Registry No. N_2H_4, 302-01-2; HNO_3, 7697-37-2; Fe, 7439-89-6.

Contribution from the Department of Chemistry, University of Pittsburgh, Pittsburgh, Pennsylvania 15260

Characterization of *o*-Phenanthroline and 2,2′-Bipyridine Complexes by Laser Mass Spectrometry

K. Balasanmugam, Robert J. Day,† and David M. Hercules*

Received January 18, 1985

A series of *o*-phenanthroline (*o*-phen) and 2,2′-bipyridine (bpy) metal complexes has been studied by using laser mass spectrometry (LMS). The molecular cation is observed in the positive ion spectra for the tetracoordinated complexes $[Ag(L)_2]NO_3$, $[Cu(L)_2]_2SO_4 \cdot 5H_2O$, $[Cu(L)_2]SO_4$, and $[Tl(L)_2](ClO_4)$, where L = bpy or *o*-phen. Structurally significant fragment ions (ML_2^+, ML^+, M^+, LH^+) are also observed. The hexacoordinate complexes $[M(L)_3]Cl_2$ and $[Fe(L)_3](ClO_4)_2$, where L = bpy or *o*-phen and M = Ni, Co, or Ru, show molecular cations in the positive ion spectra; $[Mn(bpy)_3]Br_2$ does not. Generally, fragment ions such as ML_3^+, ML_2X^+, ML_2^+, MLX^+, ML^+, and $(L + H)^+$ are observed, where X = halogen. Complexes such as $[M(o\text{-phen})_2(H_2O)_4](ClO_4)_2 \cdot 2o\text{-phen}$, where M = Ba or Pb, show ions having four ligands, e.g. $ML_4ClO_4^+$. The effect of anion on the fragmentation pattern of transition-metal complexes was studied with $[Ni(bpy)_3]X_2$ where $X = Cl^-$, Br^-, I^-, ClO_4^-, or SCN^-. Molecular cations were observed for all nickel complexes. The fragmentation patterns were similar for halide analogues. Ions arising from ion–molecule reactions from the dissociated products of ClO_4^- and CNS^- are observed. The negative ion LMS spectra of all complexes provide information about the anion and the formal oxidation state of the central metal atom.

Introduction

The mass spectrometry of coordination compounds is of interest because of their use in catalysis and chemical analysis.[1-3] Because many coordination compounds are involatile and thermally labile, analysis by mass spectrometry has been limited. Conventional mass spectrometry[4,5] has been used with limited success; field desorption (FD) has been applied to some inorganic complexes.[6-9] Though fast atom bombardment (FAB) is widely used for the

† Present address: IBM System Products Division, Endicott, NY 13760.

(1) Schilt, A. A. "Analytical Applications of 1,10-Phenanthroline and Related Compounds"; Pergamon Press: Oxford, England, 1969.
(2) Hughes, M. C.; Macero, D. J. *Inorg. Chem.* **1976**, *15*, 2040–2044.
(3) Kepert, D. L. "Inorganic Stereochemistry"; Springer-Verlag: Berlin, Heidelberg, 1982.
(4) Indrichan, K. M.; Gerbelen, N. V. *Zh. Neorg. Khim.* **1981**, *26*, 291–301; *Russ. J. Inorg. Chem. (Engl. Transl.)* **1981**, *26*, 157–163.

0020-1669/85/1324-4477$01.50/0